Materials Science & Engineering C 116 (2020) 111178

Contents lists available at ScienceDirect

Materials Science & Engineering C

journal homepage: www.elsevier.com/locate/msec

Development of brushite particles synthesized in the presence of acidic monomers for dental applications

Marina D.S. Chiari[a], Marcela C. Rodrigues[b], Mirella F.C. Pinto[a], Douglas N. Vieira[a], Flávio M. Vichi[c], Oscar Vega[d], Wojciech Chrzanowski[e], Noriyuki Nagaoka[f], Roberto R. Braga[a,*]

[a] University of São Paulo, Department of Biomaterials and Oral Biology, School of Dentistry, São Paulo, Brazil
[b] Cruzeiro do Sul University, São Paulo, São Paulo, Brazil
[c] University of São Paulo, Department of Fundamental Chemistry, Institute of Chemistry, São Paulo, Brazil
[d] Nuclear and Energy Research Institute, Center for Chemical and Environmental Technology, São Paulo, Brazil
[e] The University of Sydney, School of Pharmacy, Sydney, Australia
[f] Okayama University Graduate School of Medicine, Dentistry and Pharmaceutical Sciences, Okayama City, Okayama, Japan

ARTICLE INFO

Keywords:
Calcium phosphate
Resins composites
Mechanical properties
Ion release

ABSTRACT

Objectives: To synthesize and characterize brushite particles in the presence of acidic monomers (acrylic acid/AA, citric acid/CA, and methacryloyloxyethyl phosphate/MOEP) and evaluate the effect of these particles on degree of conversion (DC), flexural strength/modulus (FS/FM) and ion release of experimental composites.
Methods: Particles were synthesized by co-precipitation with monomers added to the phosphate precursor solution and characterized for monomer content, size and morphology. Composites containing 20 vol% brushite and 40 vol% reinforcing glass were tested for DC, FS and FM (after 24 h and 60 d in water), and 60-day ion release. Data were subjected to ANOVA/Tukey tests (DC) or Kruskal–Wallis/Dunn tests (FS and FM, alpha: 5%).
Results: The presence of acidic monomers affected particle morphology. Monomer content on the particles was low (0.1–1.4% by mass). Composites presented similar DC. For FS/24 h, only the composite containing DCPD_AA was statistically similar to the composite containing 60 vol% of reinforcing glass (without brushite, "control"). After 60 days, all brushite-containing materials showed similar FS, statistically lower than the control composite ($p < 0.01$). Composites containing DCPD_AA, DCPD_MOEP or DCPD_U ("unmodified") showed statistically similar FM/24 h, higher than the control composite. After prolonged immersion, all composites were similar to the control composite, except DCPD_AA. Cumulative ion release ranged from 21 ppm to 28 ppm (calcium) and 9 ppm to 17 ppm (phosphate). Statistically significant reductions in ion release between 15 and 60 days were detected only for the composite containing DCPD_MOEP.
Significance: Acidic monomers added to the synthesis affected brushite particle morphology. After 60-day storage in water, composite strength was similar among all brushite-containing composites. Ion release was sustained for 60 days and it was not affected by particle morphology.

1. Introduction

Experimental resin composites containing calcium orthophosphate (CaP) particles were shown to promote *in vitro* remineralization of non-cavitated enamel lesions [1–3], as well as to inhibit *in situ* caries development in the presence of biofilm [4]. Unfortunately, the addition of CaP particles in the composite leads to significant reductions in strength and fracture toughness [5,6] and increased wear [7], which may limit its use in stress bearing areas such as large, multi-surface restorations. The reduction in mechanical properties occurs due to the fact that CaP particles are usually added at the expense of reinforcing filler content and they lack the cohesive strength to act as toughening agents. Moreover, the absence of chemical interaction between CaP particles and the organic matrix increase the risk of crack initiation and propagation through the matrix-particle boundaries [5,6].

In order to control particle growth and provide reactive sites for chemical bonding with the resin matrix, CaP particles can have their surface modified *via* functionalization with carboxylic acids [8], ethylene glycol dimethacrylate (EGDMA) derivatives [9–11] or silanes [12]. Resin-based materials containing brushite particles (dicalcium phosphate

* Corresponding author at: Department of Biomaterials and Oral Biology, University of São Paulo School of Dentistry, Av. Prof. Lineu Prestes, 2227, São Paulo, SP 05508-000, Brazil.
E-mail address: rrbraga@usp.br (R.R. Braga).

https://doi.org/10.1016/j.msec.2020.111178
Received 27 March 2020; Received in revised form 4 June 2020; Accepted 8 June 2020
Available online 17 June 2020

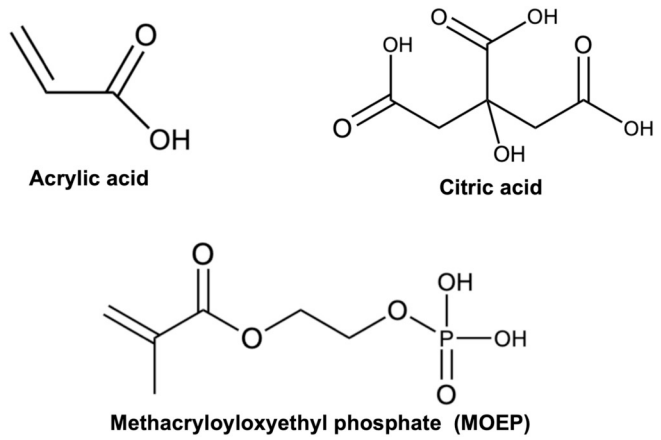

Fig. 1. Structural formulas of the acidic monomers used as functionalizing agents for the brushite particles.

dihydrate, DCPD, $CaHPO_4.2H_2O$) functionalized with ethylene glycol dimethacrylate (EGDMA) monomers were tested in a series of studies [9–11,13–16]. The number of EG units in the spacer group (*i.e.,* di-, -tri- or tetra-ethylene glycol dimethacrylate) was shown to influence the mass fraction of monomer retained on the particles [17]. However, particle size and morphology were not significantly affected by functionalization with EGDMA monomers, which may explain the overall modest (though statistically significant) improvements in fracture strength verified in resin-based composites containing functionalized particles in comparison to non-functionalized brushite [10,11,13–15].

Carboxylic acids (malic, citric, acrylic and methacrylic acid) have been tested as coupling agents between hydroxyapatite (HA) and dimethacrylate-based matrices [8,18,19]. Improved mechanical properties were reported for composites containing micrometric HA functionalized with acrylic acid (in relation to the control containing non-functionalized particles) likely due to binding of ionizable carboxylic groups to the particle surface and the presence of a vinyl group that can copolymerize with the organic matrix [8,19]. Citric acid (Fig. 1) does not present polymerizable groups, but it was shown to inhibit crystal growth and reduce agglomeration when added to one of the ion precursor solutions in the synthesis of HA particles [20,21]. Similar to acrylic acid, methacrylate monomers containing phosphoric acid groups also present negatively charged sites, potentially capable of binding to Ca^{2+} and reducing particle agglomeration. Methacryloyloxyethyl phosphate (MOEP, Fig. 1), for example, was tested for its CaP nucleation potential *in vitro* [22]. Its molecular structure is similar to EGDMA, but instead of a second methacrylate, it presents a phosphate end group.

Based on the above, the present study aimed to investigate the effects of different acidic monomers on the synthesis of brushite particles and test these particles as ion-releasing fillers in experimental resin-based dental restorative composites. Experimental composites were evaluated for degree of conversion, mechanical properties (biaxial flexural strength and flexural modulus). Composite degradation was indirectly accessed by comparing the mechanical properties after 24 h and 60 days in water. The work hypothesis was that negatively charged organic molecules (such as citric acid, acrylic acid and MOEP) would contribute to reduce particle size, while those presenting polymerizable vinyl groups (acrylic acid and MOEP) would present the additional benefit of a establishing a stronger interface between the brushite particles and the composite resin matrix.

2. Material and methods

2.1. Particles syntheses

Brushite particles (hereafter referred as DCPD) were synthesized by co-precipitation using calcium nitrate [$Ca(NO_3)_2.4H_2O$] and ammonium hydrogen phosphate [$(NH_4)_2HPO_4$] solutions (1 mol·L^{-1}) as precursors (all chemicals from Sigma-Aldrich, St. Louis, MO). For the syntheses of functionalized particles, citric acid (CA), acrylic acid (AA) or MOEP monomers (Fig. 1) were added to the phosphate solution at molar ratios of 0.1:1.0 (CA) or 0.3:1.0 (AA and MOEP). Monomer concentrations were defined in preliminary tests and available literature [23]. The calcium nitrate solution was added drop-wise to the ammonium dihydrogen phosphate/monomer solution using a peristaltic pump (9 mL/min) under constant stirring, at room temperature. Particle suspension was kept under stirring for 3 h. The pH of the receiving solution was monitored during the entire procedure. Reaction by-product (ammonium nitrate, NH_4NO_3) and unbound monomer were removed by five cycles of rinsing in deionized water and centrifugation (1077*g*) at −4 °C (Thermo Fisher Scientific, Asheville, NC, USA). The resulting gel was freeze-dried until a white powder was obtained.

2.2. Particle characterization

The calcium orthophosphate phase obtained in the synthesis was identified by X-ray diffractometry (XRD), using nickel filtered CuKa radiation at 40 kV and 30 mA. The equipment geometry was θ/2θ and continuous readings were taken from 10° to 60° at 0.05° intervals and 2°/min (XRD-7000 Maxima, Shimadzu, Kyoto, Japan). Monomer mass fraction on the particles was determined by carbon infrared absorption (CS-400 Carbon analyzer, LECO Corp., St. Joseph, Michigan, USA), with resolution of 2 μg of carbon *per* gram of the sample. The carbon monoxide (CO) formed by the combustion of approximately 1 g of material in oxygen atmosphere was converted to CO_2 and quantified in infrared cells [24,25]. Particles were also characterized in terms of true density in a helium pycnometer (Ultrapyc 1200e, Quantachrome Instruments, Boynton Beach, FL, USA), size distribution (*i.e.*, equivalent spherical diameter) using laser scattering (Mastersizer 2000, Malvern Instruments Ltd., Malvern, UK), and zeta potential (Zetasizer, Malvern). Finally, particle morphology was observed under a scanning electron microscope (Quanta FEG600, Eindhoven, The Netherlands).

2.3. Composite formulation

A series of five photocurable composites was prepared with the organic phase containing equimolar amounts of BisGMA (2,2-bis[4-(2-hydroxy-3-methacryloxypropoxy)phenyl]-propane) and TEGDMA (triethylene glycol dimethacrylate). Camphorquinone and ethyl-4-dimethylamino benzoate (EDMAB, all components from Sigma-Aldrich) were added as photoinitiators (0.5% mass fraction each). Inorganic fraction was constituted by 40 vol% of silanated barium glass (D_{50}: 2 μm) and 20 vol% of DCPD particles. A composite containing 60 vol% of barium glass was used as control. Components were mechanically mixed under vacuum (Speedmixer DAC 150.1 FVZ−K, FlackTek Inc., Landrum, SC, USA) and kept under refrigeration until 2 h before use.

2.4. Degree of conversion

Degree of conversion (DC, $n = 5$) was determined using near-FTIR (Fourier transform infrared, Vertex 70, Bruker Optics, Germany). The uncured material was inserted in a silicone mold (5 × 1 mm), pressed between two glass slides and a first spectrum was obtained (32 scans, 4 cm^{-1} resolution). After photoactivation (24 J/cm^2, Bluephase, Ivoclar-Vivadent, Schaan, Liechtenstein,) and dry-storage for 24 h at 37 °C, a new spectrum was collected in a similar manner. DC was calculated based on the ratio between the intensities of the absorption band located at 6165 cm^{-1} (corresponding to the aliphatic = CH group), according to the formula:

$$DC = \left(1 - \frac{polymerized}{non - polymerized}\right) \times 100$$

2.5. Mechanical properties

Disk-shaped specimens (12 × 1 mm, $n = 12$) were made using a stainless steel split mold, each quadrant being photoactivated for 20 s (24 J/cm^2 per quadrant, Bluephase, Ivoclar Vivadent). The specimens were fractured after 24 h or 60 days of storage in deionized water at 37 °C on a "piston on three spheres" testing accessory positioned under the actuator of a universal testing machine (Instron model 5565, Instron Corp, Canton, MA, USA). The center of the specimen was loaded at a crosshead speed of 0.5 mm/min until failure. Deflection at the center of the specimen was monitored by a contact transducer (model W-E401-E, Instron). Biaxial flexural strength (σ_{BFS}, in MPa) was calculated using the equations below:

$$\sigma_{BFS} = \frac{-0.2387P\,(X - Y)}{b^2}$$

$$X = (1 + \upsilon)In\left(\frac{r_2}{r_3}\right)^2 + \left[\left(\frac{1 - \upsilon}{2}\right)\right]\left(\frac{r_2}{r_3}\right)^2$$

$$Y = (1 + \upsilon)\left[1 + In\left(\frac{r_1}{r_3}\right)^2\right] + (1 - \upsilon)\left(\frac{r_1}{r_3}\right)^2$$

where P is the failure load (in Newtons); b is the specimen thickness (in mm); ν is the specimen Poisson's ratio (0.3); r_1 is the radius of the circle where the spheres were positioned (5.0 mm); r_2 is the loading piston radius (0.6 mm); r_3 is the specimen radius (in mm). Flexural modulus (FM, in GPa) was calculated according to the following equation:

$$FM = \frac{\beta P a^2}{\omega h^3}$$

where β is a constant related to the deflection at the center of the disk (0.509), P is the load (in Newtons), a is the disk radius (in mm), ω is the deflection corresponding to P and h is the disk thickness (in mm).

2.6. Ion release

Disk-shaped specimens (5 × 1 mm, $n = 5$) were prepared using a silicone mold, with a single 20-s irradiation (24 J/cm^2, Bluephase, Ivoclar Vivadent). After 24 h storage at 37 °C the specimens were immersed individually in 5 mL of NaCl solution (133 mol·L^{-1}) buffered to pH = 7 with 50 mmol/L HEPES solution (50 mmol·L^{-1}). Specimens were transferred to vials containing fresh medium every two weeks, and calcium and phosphorous released concentrations up to 60 days were quantified in the retrieved solution using inductively coupled plasma-optical emission spectrometry (ICP-OES, 700, Agilent Technologies, Santa Clara, CA, USA).

2.7. Atomic force microscopy

Particle surface topography was observed using atomic force microscopy (AFM; XE-70, Park Systems, Suwon, Korea). Images of the surface were recorded in non-contact (*i.e.*, tapping) mode using a silicon tip (force constant: 42 N.m^{-1}, resonance frequency: 32 KHz) at 0.5 Hz scan rate. Scans were performed in areas ranging from 25 × 25 μm to 1 × 1 μm. Images were obtained at resolutions of 256 × 256 pixels or 512 × 512 pixels (for areas smaller than 5 × 5 μm).

2.8. Statistical analysis

Data sets were subjected to normality and homoscedasticity tests (Levine and Anderson-Darling tests, respectively). DC was analyzed using one-way ANOVA and Tukey test for multiple comparisons. Due to the lack of homoscedasticity, FS, FM and ion release data were analyzed using non-parametric tests (Kruskal–Wallis and Dunn's test for pair-wise comparisons). In all cases, the global significance level was 5%.

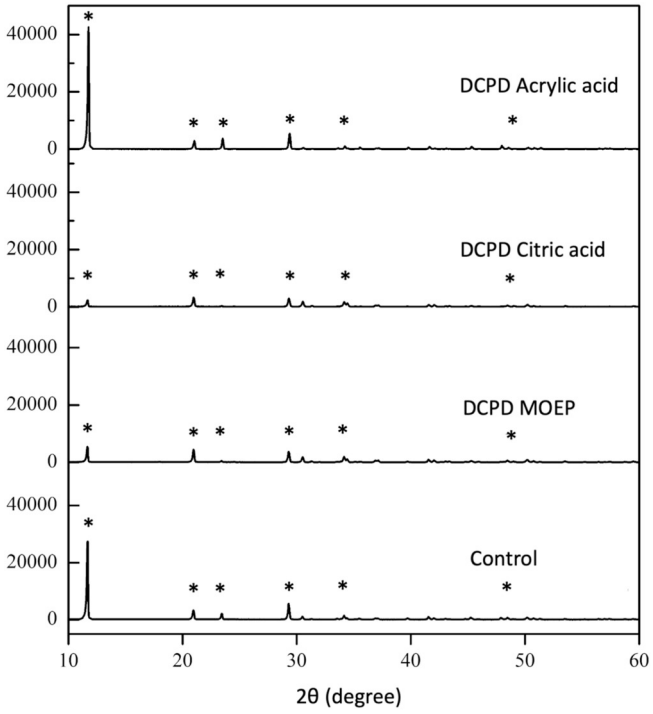

Fig. 2. Diffractograms of the particles synthesized in this study. Asterisks indicate diffraction peaks characteristic of DCPD. "Control" refers to the particles synthesized without added monomers (DCPD_U). Notice that the same interval was used in the y-axis for all the diffractograms to evidence differences in crystal size.

3. Results

3.1. Particles characterization

The diffractograms in Fig. 2 show the presence of peaks characteristic of the DCPD crystalline structure [26]. The four diffractograms are shown using the same scale in the y-axis to evidence the lower intensity of the peaks (*i.e.*, lower crystallite size) for particles synthesized in the presence of citric acid (DCPD_CA) and MOEP (DCPD_MOEP) in relation to the control particles ("unmodified", DCPD_U). Characteristics of the synthesized particles are shown in Table 1. Monomer retention on the particle surface was low, which agrees with the similar density values recorded for particles obtained in all synthesis conditions. In relation to DCPD_U, particles synthesized in the presence of CA showed lower median size, while the use of MOEP resulted in larger particles. Zeta potential varied within a relatively small range.

Images of the particles obtained in the scanning electron microscope are shown in Fig. 3. DCPD_U and particles synthesized in the presence of acrylic acid (DCPD_AA) presented similar morphology, with elongated, thin plates. DCPD_MOEP were also plate-like, although thicker and less elongated, with several large flower-like clusters (as shown in Fig. 3C). The addition of citric acid in the synthesis resulted in clusters of needle-like particles. Examples of AFM images of the DCPD particles are shown in Fig. 4. The 3D topography images (top row) of DCPD_U, DCPD_AA and DCPD_MOEP evidence the stacking of the plates, each one with approximately 120 nm in thickness. The bottom row shows the superimposed of topography and phase contrast images. DCPD_U and DCPD_AA particles show no contrast (*i.e.*, uniform color throughout the surface), indicative of uniform stiffness throughout the surface. On the other hand, DCPD_MOEP and DCPD_CA show some phase contrast, suggesting the presence of a less stiff layer of monomer on the surface.

Table 1
Characterization of the particles synthesized in the study.

Functionalizing agent	Organic content (% mass fraction)	Density (g/cm^3)	Particle size (D_{50}, in μm)	Zeta Potential (mV)
Acrylic acid (DCPD_AA)	0.1	2.41	21	−0.9
Citric acid (DCPD_CA)	1.4	2.45	10	−10.6
MOEP (DCPD_MOEP)	0.3	2.38	38	−14.2
Unmodified (DCPD_U)	Not applicable	2.53	21	−5.2

3.2. DCPD-containing resin materials

For DC, no statistically significant differences were detected among composites, with values ranging from 76% to 82% ($p > 0.05$, Table 2). Flexural properties of the experimental composites are shown in Fig. 5. In relation to the glass-only composite, the replacement of 20 vol% of barium glass particles by DCPD in a 60 vol% total inorganic content resulted in reduced initial strength between 16% and 32%. Only the composite containing DCPD_AA presented flexural strength similar to the glass-only composite and also statistically higher than the composite with DCPD_U after 24 h ($p < 0.01$). Composites containing DCPD_CA and DCPD_MOEP were statistically similar to the material with DCPD_U. After 60 days in water, all composites presented statistically significant decreases in strength (between 23% and 35%) and no differences were observed among DCPD-containing materials, regardless of the use of acidic monomers in the synthesis ($p > 0.05$).

The presence of DCPD particles significantly increased composite flexural modulus in relation to the control, except for those containing DCPD_CA. Prolonged water storage did not affect the flexural modulus for the glass-only composite and the material containing DCPD_CA. The other three composites presented statistically significant reductions, between 15% and 32%. Except for the composite containing DCPD_AA, all the other DCPD-containing composites showed flexural moduli statistically similar to the glass-only composite after 60 days in water ($p < 0.05$). A cross-sectional view of the microstructure of the composite containing DCPD_U is shown in Fig. 6. It is possible to observe the homogeneous dispersion of the DCPD plates (dark grey) among the barium glass particles (light grey). Interestingly, plates are fairly well-oriented perpendicularly to the disk-shaped specimen axis.

Examples of 3D height topographic images of composite surface observed under the atomic force microscope are shown in Fig. 7. The aspect of the DCPD_U particles in the composite (Fig. 7A) did not differ to what was presented in Fig. 4, with mostly flat surfaces and well-defined corners, surrounded by smaller glass particles. For the composites containing DCPD particles synthesized in the presence of acidic monomers and for the silanized glass (shown in Fig. 7D), corners are not well-defined. For the composite containing DCPD_MOEP was difficult to identify the particle contour (Fig. 7C). Phase contrast images (not shown) suggest the presence of a resin layer on and accumulated around the functionalized glass and particles synthesized in the presence of acidic monomers.

Calcium release at the first 15 days was statistically similar among composites, ranging from 8 ppm to 10 ppm (Fig. 8, left). Statistically significant reductions were observed after 30 days (for composite containing DCPD_U and DCPD_AA) or 45 days (DCPD_CA and DCPD_MOEP). At 60 days, calcium release was reduced to 3–5 ppm, and the only statistically significant difference was between the composites with DCPD_CA and DCPD_MOEP ($p < 0.05$). Phosphate release was

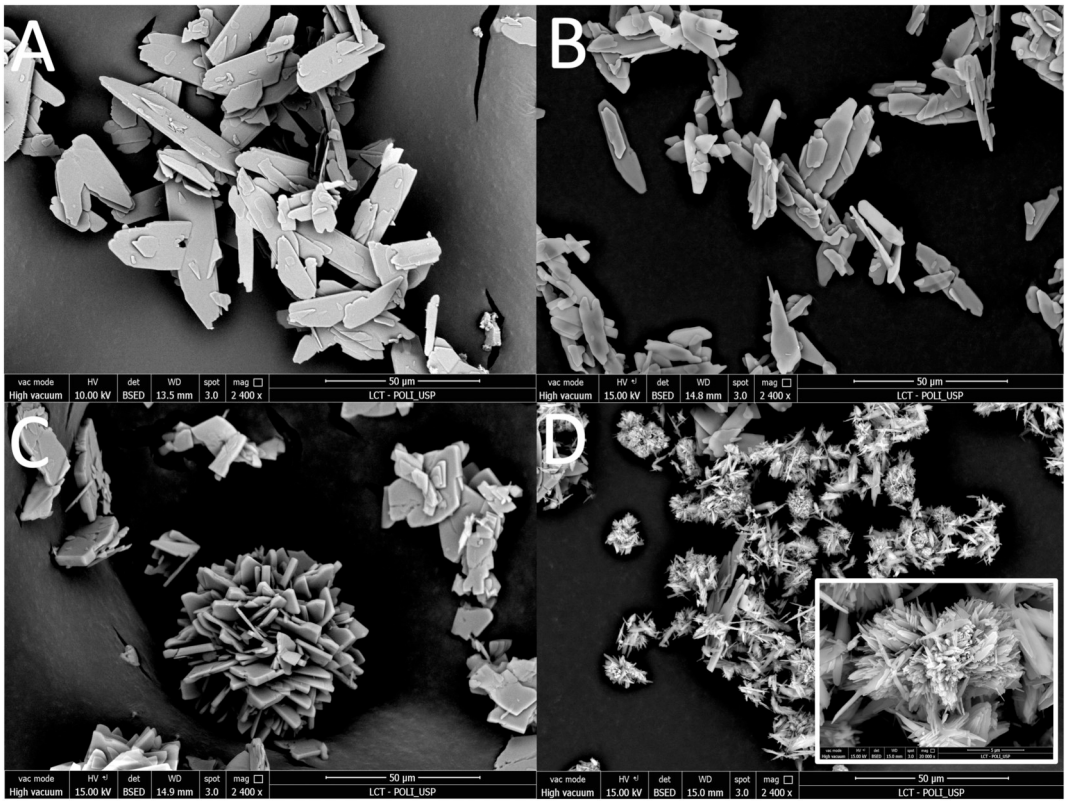

Fig. 3. Scanning electron microscopy (SEM) images showing particles obtained with different syntheses conditions. (A) unmodified (DCPD_U), (B) acrylic acid (DCPD_AA), (C) MOEP (DCPD_MOEP), (D) citric acid (DCPD_CA, with an inset at higher magnification).

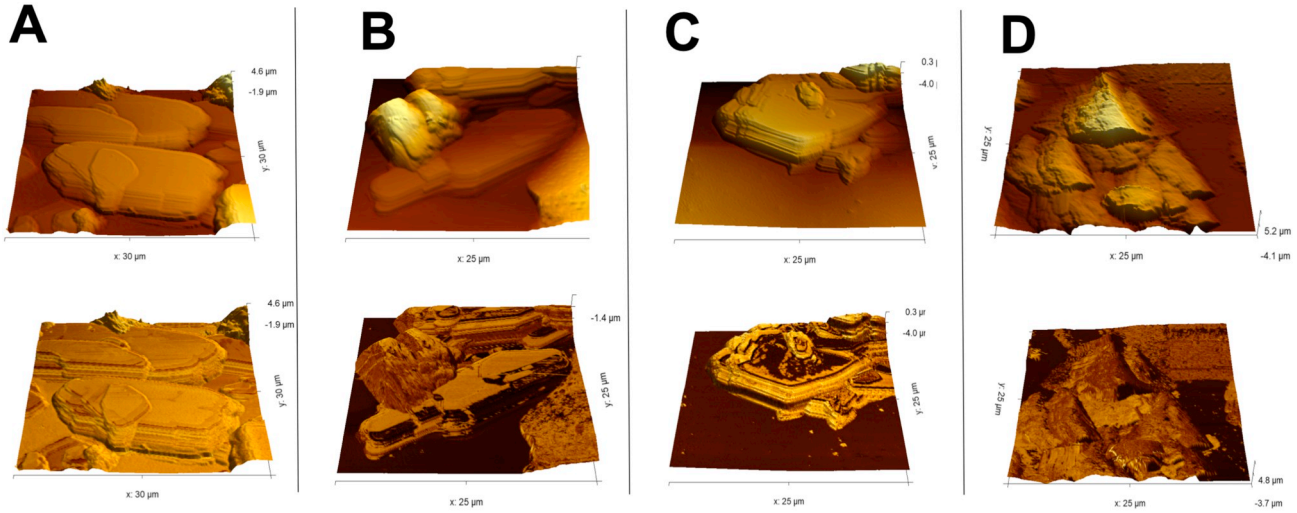

Fig. 4. Examples of atomic force microscopy images of the DCPD particles synthesized in the study (top row: 3D topography, bottom row: topography/phase contrast overlay). A: DCPD_U, B: DCPD_AA, C: DCPD_MOEP, D: DCPD_CA.

Table 2
Means and standard deviations for degree of conversion (in %) of experimental composites containing 40 vol% of barium glass and 20 vol% of DCPD particles synthesized in the presence of acrylic acid, citric acid, MOEP or not ("unmodified"). An experimental composite containing 60 vol% of silanated barium glass was used as control. Similar letters indicate lack of statistically significant differences (ANOVA/Tukey tests, $p > 0.05$).

Composite	Degree of conversion (%)	
Without DCPD (glass only)	77.7 (0.7) A	
With DCPD	80.1 (1.2) A	Acrylic acid (DCPD_AA)
	76.8 (0.6) A	Citric acid (DCPD_CA)
	82.6 (6.6) A	MOEP (DCPD_MOEP)
	80.1 (4.4) A	Unmodified (DCPD_U)

lower than calcium (Fig. 8, right). In general, similar concentrations were observed among the materials for the same period, except for the first 15 days when materials with particles synthesized in the presence of acidic monomers presented a numerical tendency to release higher phosphate concentrations than the group with DCPD_U. Materials containing DCPD_AA and DCPD_CA presented the highest cumulative phosphate release (15 ppm and 18 ppm, respectively) and no statistical reductions were observed for both groups between the storage periods.

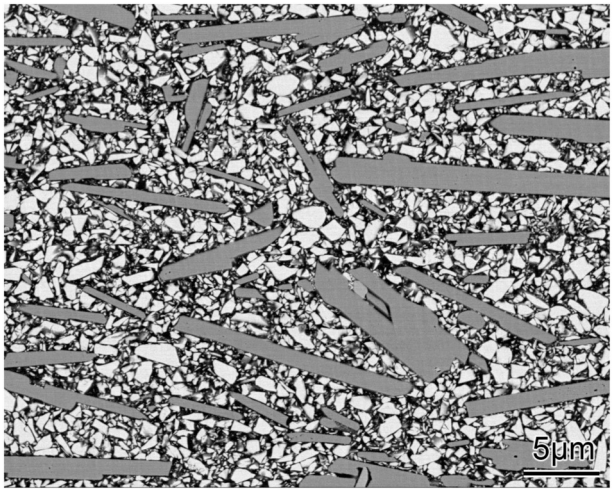

Fig. 6. Example of scanning electron microscopy (SEM) image of a polished cross sectional surface of the composite containing 20 vol% of DCPD_U and 40 vol% of silanated barium glass.

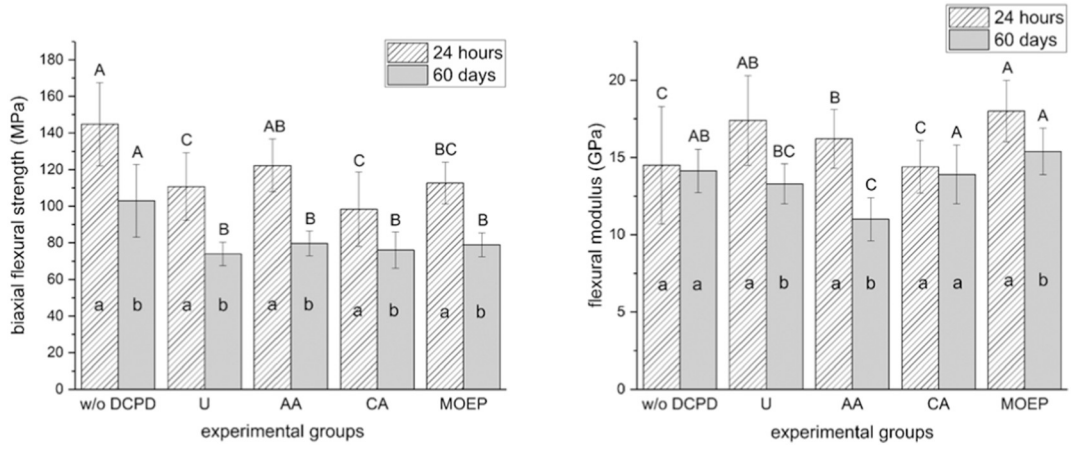

Fig. 5. Means and standard deviations for biaxial flexural strength (left) and flexural modulus (right) of resin-based materials containing 40 vol% of reinforcing glass and 20 vol% of DCPD particles synthesized with acrylic acid (AA), citric acid (CA), MOEP or without added monomers (U). A composite containing 60 vol% of reinforcing glass ("w/o DCPD") was also tested. Similar upper-case letters indicate lack of statistically significant differences among materials for the same storage time. Similar lower-case letters indicate lack of statistically significant differences among storage times for the same material (Kruskal–Wallis/Dunn tests, $p > 0.05$).

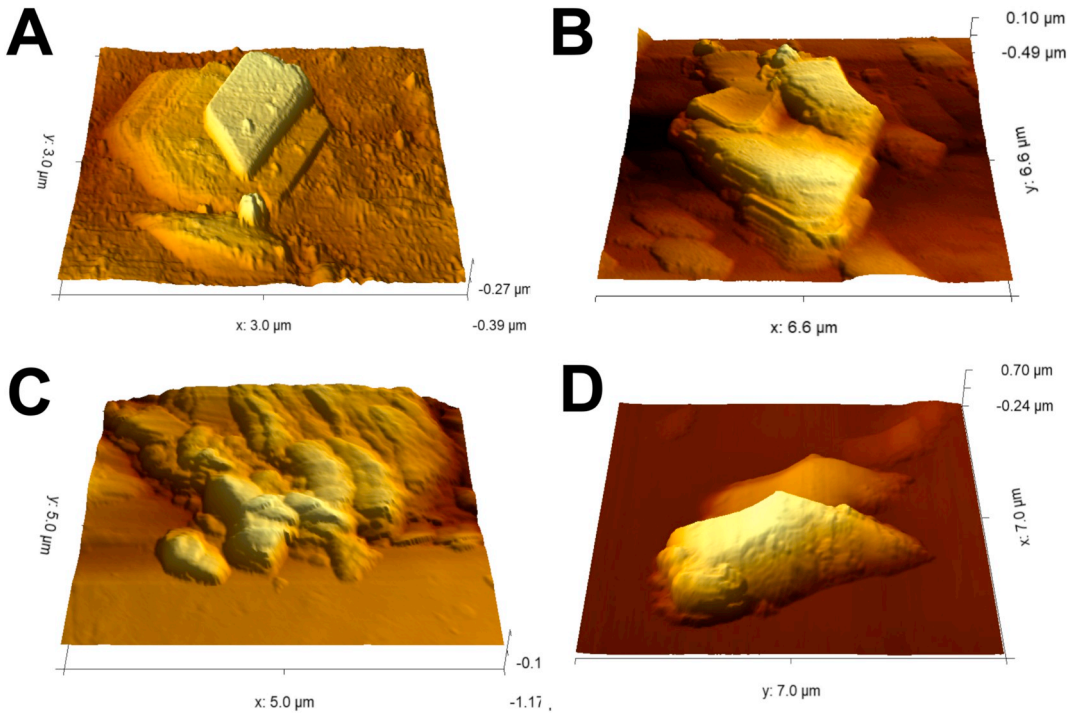

Fig. 7. Examples of atomic force microscopy topographic images showing DCPD (A: DCPD_U, B: DCPD_AA, C: DCPD_MOEP) and reinforcing glass particles (D) on the surface of cured composite specimens.

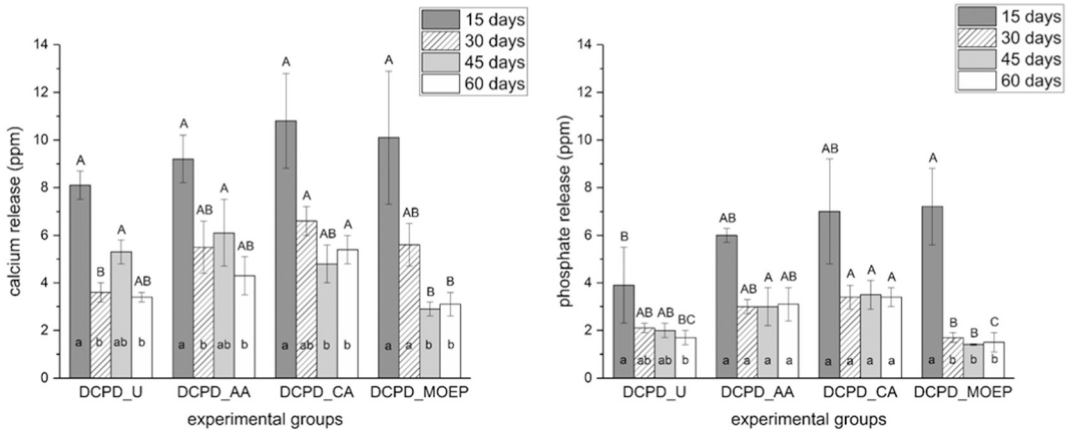

Fig. 8. Means and standard deviations for calcium (left) and phosphorous (right) release from composites containing 20 vol% of DCPD particles and 40 vol% of barium glass particles. Similar upper-case letters indicate lack of statistically significant differences among materials for the same storage time. Similar lower-case letters indicate lack of statistically significant differences among storage times for the same material (Kruskal–Wallis/Dunn tests, $p > 0.05$).

The cumulative release for the materials containing DCPD_U or DCPD_MOEP was similar (9 ppm and 12 ppm, respectively) and reductions between periods were only observed between 15 and 30 days.

4. Discussion

4.1. Particles characterization

DCPD particles have been tested as ion-releasing filler in resin-based materials in previous studies [5,10,11,13–16,27]. Its refractive index (1.54–1.55) is similar to the barium glass used as reinforcement in dental composites, as well as to the resin phase [28]. Matching the refractive indices of the particles with the resin phase is fundamental to maximize light transmission through the material during photoactivation and also to mimic the optical behavior of the tooth structure. Furthermore, compared to other calcium orthophosphate phases, DCPD presents an intermediate solubility [29], which may be advantageous in terms of ion release.

Among the three acidic monomers added in the synthesis, citric acid and MOEP substantially changed particle morphology, while acrylic acid did not. DCPD_U and DCPD_AA presented the typical plate-like morphology, already verified in previous studies [11,30,31]. On the other hand, DCPD_CA showed acicular crystals, explained by the ability of citrate ions to inhibit crystal growth in a specific axis, inducing the formation of needle-shape crystals [32]. The presence of MOEP resulted in thick plates, less elongated than DCPD_U, some of them arranged as large flower-like clusters. Also, the more negative zeta potential values presented by DCPD_MOEP and DCPD_CA indicate the presence of residual monomers, creating a slight excess of negative sites on the particles surface [33].

In spite of their influence on particle morphology, retention of acidic monomers on the surface of the particles was very small. A

possible explanation for this finding would be related to the pH conditions during the synthesis. The pH of the reaction medium varied from 6.2–6.6 at the beginning of the co-precipitation to 4.1–4.5 at the end of the stirring period. Slightly acidic conditions are necessary for the formation of DCPD [34]. However, within this range, monomer acidic groups were not sufficiently dissociated, which may have compromised their interaction with calcium ions in solution. Citric acid presents three carboxyl groups (-COOH) with dissociation constants (pKa) of 3.1, 4.7 and 6.4. As such, at pH 6.5, the dissociation percentage expected for each carboxylic group is 77% (HA^-), 22% (HA^{2-}) and 0.2% (HA^{3-}), as calculated using CurTiPot software (http://www.iq.usp.br/gutz/Curtipot.html); however, as the pH of the reaction medium becomes more acidic, dissociation rates decrease. At pH 4.5 the expected dissociations are 50% (HA^-), 46% (HA^{2-}) and 1.6% (HA^{3-}). In either case, citric acid was only partially dissociated. Acrylic acid pKa is 4.25. At the beginning of the synthesis, its carboxylic group is expected to be almost fully dissociated (99.7%), but the dissociation reduced to 64% as the pH became more acidic. As MOEP presents pKa_1 = 7.21 and pKa_2 = 12.67, the dissociation of the –OH groups during the synthesis was small: 25% (pH 6.5) and 0.4% (pH 4.5). Thus, it could be hypothesized that monomer retention on the particle would have been effective if pH during synthesis was kept at the highest possible value necessary for DCPD formation (*i.e.*, pH = 6). Despite the lack of an effective functionalization, atomic force microscopy showed evidence of areas with lower stiffness at the surface of DCPD_MOEP and DCPD_CA, suggestive of the presence of residual monomer.

4.2. Flexural properties of DCPD-containing composites

The lack of statistically significant differences between groups for degree of conversion was expected based in previous reports [5,11,14] and it is important to exclude the influence of polymer network characteristics on the evaluated properties. Flexural strength after 24 h ranged from 98 MPa (composite with DCPD_CA) to 145 MPa (glass-only composite). It is noteworthy that the difference in particle size (DCPD_U: 21 μm; DCPD_CA: 10 μm) did not affect strength results. On the other hand, the composite containing DCPD_AA and DCPD_MOEP presented similar strength, but only the former was similar to the control (122 MPa). Probably, the thin plate morphology of particles obtained with the addition of acrylic acid resulted in less defects within the resin matrix when compared to thicker plates and clusters presented by DCPD_MOEP. Moreover, the irregular shape of the DCPD_CA and DCPD_MOEP may contribute for stress concentration at the particle-matrix interface [35] and facilitate crack propagation [36]. However, even without a significant amount of monomer retained on the particles, some residual monomer may have persisted, as suggested by their similar aspect compared to that of the silanized glass particle, when composites were observed under the AFM. Their irregular edges differ from those of DCPD_U and DCPD_CA, which show well-defined edges and flat surfaces.

After 60 days in water, all composites presented statistically significant reductions in strength (DCPD-containing composites: 23–35%, glass-only composite: 28%), which can be ascribe to the hydrolysis of the resin matrix [37]. It is important to notice that the replacement of 20 vol% of glass particles with DCPD did not contribute to a more severe reduction in fracture strength, even considering that resin matrix hydrolysis may be more severe due to the increased interparticle spacing as a result of the presence of large DCPD plates. Also, transit of fluids at the DCPD-matrix interface is facilitated by the absence of chemical interaction, in agreement with previous results [38].

The glass-only composite and that containing DCPD_CA showed the lowest elastic modulus, while the composite with DCPD_MOEP presented the highest values. Composite stiffness is related to filler content and particle-particle interaction [39]. Though the replacement of small glass particles by large DCPD particles leads to an increase in interparticle spacing which may reduce composite stiffness, this relationship is not linear [38]. Furthermore, is modulated by particle morphology. In the present study, the presence of large DCPD particles had a positive effect on the flexural modulus after 24 h. Additionally, the lack of statistical difference between the materials containing DCPD_U and DCPD_MOEP or DCPD_AA confirms that the chemical bond between the organic matrix and inorganic phase is not a determining factor for material stiffness [40]. Different from what was observed for flexural strength, after 60 days statistically significant reductions were observed only for composites containing large plate-like DCPD particles (namely, DCPD_U, DCPD_AA and DCPD_MOEP), which may be the result of increased transit of fluids (and consequent matrix plasticization) resulting from larger interparticle spacing. The fact that the composite containing DCPD_CA (with the smallest size among the synthesized particles) did not show a significant reduction in modulus and also presented the lowest percent reduction in strength after water storage supports this hypothesis. It is important to highlight, though, that (with one exception) flexural modulus of DCPD-containing composites after prolonged water storage was similar to the glass-only material.

4.3. Ion release

Cumulative ion release after 60 days ranged from 21 ppm to 28 ppm (Ca^{2+}), and between 9 ppm and 17 ppm (HPO_4^{2-}), and are similar to concentrations reported in previous studies [12,41]. Overall, with very few exceptions, ion release was not affected by the type of DCPD particles used in the composite formulation. However, particles synthesized with acidic monomers presented a numerical tendency to release higher concentrations in comparison to DCPD_U at 15 days. It could be speculated that particles with residual monomer become more hydrophilic, increasing the transit of fluids at the interface in relation to the material containing DCPD_U, somewhat facilitating ion release initially [42]. Noteworthy, the composite with DCPD_CA showed higher calcium release (at 60 days) and phosphate release (at 30, 45 and 60 days) than the composite with DCPD_MOEP, suggesting that the small particle size of the former (and, consequently, higher surface area) had a positive effect on this variable.

It has been shown that calcium and phosphate ions released from bioactive composites in concentrations of 30 ppm and 17 ppm, respectively, were able to promote enamel remineralization *in vitro* [1]. Also, experimental composites containing 40 vol% amorphous calcium phosphate and/or tetracalcium phosphate were able to promote substantial dentin remineralization (43–48% mineral gain) after eight weeks of cyclic demineralization/remineralization treatment, with calcium concentrations of approximately 47 ppm being released after 56 days in pH 7.0 [43].

In summary, the incorporation of acidic monomers in the DCPD synthesis changed particle morphology. Composite initial flexural strength values suggest that particles synthesized with acrylic acid and MOEP presented a more favorable morphology, in comparison to those synthesized in the presence of citric acid and the unmodified DCPD. Similarly, initial flexural modulus was improved by the presence of large DCPD particles (*i.e.*, DCPD_U, DCPD_AA and DCPD_MOEP). However, these effects were not observed after 60 days aging in water. DCPD-containing materials showed lower flexural strength in comparison to the control composite, both initially (16–32% lower strength) and after aging (22–28% lower strength), which may limit their use in load-bearing restorations. Sustained ion release was observed for 60 days, with statistically significant differences between composites containing DCPD_CA (D_{50}: 10 μm) and DCPD_MOEP (D_{50}: 38 μm). Future studies will focus on the influence of pH on DCPD particle synthesis in the presence of acidic monomers.

CRediT authorship contribution statement

Marina D.S. Chiari: Conceptualization, Investigation, Formal analysis, Writing - original draft.**Marcela C. Rodrigues:**Investigation.**Mirella F.C. Pinto:**Investigation.**Douglas N. Vieira:**Resources.**Flávio M.**

Vichi:Investigation, Resources.**Oscar Vega**:Investigation, Resources. **Wojciech Chrzanowski**:Investigation, Resources.**Noriyuki Nagaoka**: Investigation, Resources.**Roberto R. Braga**:Methodology, Project administration, Supervision, Visualization, Writing - review & editing.

Declaration of competing interest

The authors declare that they have no known competing financial interests or personal relationships that could have appeared to influence the work reported in this paper.

Acknowledgments

This study was funded by grants #2016/25971-7, #2017/06446-1 and #2016/50321-6, São Paulo Research Foundation (FAPESP), and CAPES (Coordination for the Improvement of Higher Education Personnel). Authors would like to thank FGM Dental Products for donating the glass fillers.

References

[1] S.E. Langhorst, J.N. O'Donnell, D. Skrtic, In vitro remineralization of enamel by polymeric amorphous calcium phosphate composite: quantitative microradiographic study, Dent. Mater. 25 (7) (2009) 884–891.
[2] D. Skrtic, et al., Quantitative assessment of the efficacy of amorphous calcium phosphate/methacrylate composites in remineralizing caries-like lesions artificially produced in bovine enamel, J. Dent. Res. 75 (9) (1996) 1679–1686.
[3] M.D. Weir, L.C. Chow, H.H. Xu, Remineralization of demineralized enamel via calcium phosphate nanocomposite, J. Dent. Res. 91 (10) (2012) 979–984.
[4] M.A. Melo, et al., Novel calcium phosphate nanocomposite with caries-inhibition in a human in situ model, Dent. Mater. 29 (2) (2013) 231–240.
[5] M.D. Chiari, et al., Mechanical properties and ion release from bioactive restorative composites containing glass fillers and calcium phosphate nano-structured particles, Dent. Mater. 31 (6) (2015) 726–733.
[6] H.H. Xu, J.L. Moreau, Dental glass-reinforced composite for caries inhibition: calcium phosphate ion release and mechanical properties, J Biomed Mater Res B Appl Biomater 92 (2) (2010) 332–340.
[7] J.L. Moreau, et al., Long-term mechanical durability of dental nanocomposites containing amorphous calcium phosphate nanoparticles, J Biomed Mater Res B Appl Biomater 100 (5) (2012) 1264–1273.
[8] R.W. Arcis, et al., Mechanical properties of visible light-cured resins reinforced with hydroxyapatite for dental restoration, Dent. Mater. 18 (1) (2002) 49–57.
[9] M.C. Rodrigues, et al., Calcium phosphate nanoparticles functionalized with a dimethacrylate monomer, Mater. Sci. Eng. C Mater. Biol. Appl. 45 (2014) 122–126.
[10] L.C. Natale, et al., Mechanical characterization and ion release of bioactive dental composites containing calcium phosphate particles, J. Mech. Behav. Biomed. Mater. 84 (2018) 161–167.
[11] L.C. Natale, et al., Development of calcium phosphate/ethylene glycol dimethacrylate particles for dental applications, J. Biomed Mater. Res. B Appl. Biomater. 107 (3) (2019) 708–715.
[12] H.H. Xu, M.D. Weir, L. Sun, Nanocomposites with Ca and PO_4 release: effects of reinforcement, dicalcium phosphate particle size and silanization, Dent. Mater. 23 (12) (2007) 1482–1491.
[13] Y. Alania, et al., Bioactive composites containing TEGDMA-functionalized calcium phosphate particles: degree of conversion, fracture strength and ion release evaluation, Dent. Mater. 32 (12) (2016) e374–e381.
[14] M.C. Rodrigues, et al., Polymer-based material containing calcium phosphate particles functionalized with a dimethacrylate monomer for use in restorative dentistry, J. Biomater. Appl. 31 (6) (2017) 871–877.
[15] M.C. Rodrigues, et al., Ion-releasing dental restorative composites containing functionalized brushite nanoparticles for improved mechanical strength, Dent. Mater. 34 (5) (2018) 746–755.
[16] Y. Alania, et al., In vitro remineralization of artificial enamel caries with resin composites containing calcium phosphate particles, J. Biomed. Mater. Res. B Appl. Biomater. 107 (5) (2019) 1542–1550.
[17] M.F.C. Pinto, et al., Effect of bioactive composites on microhardness of enamel exposed to carious challenge, Eur. J. Prosthodont. Restor. Dent. 26 (3) (2018) 122–128.
[18] C. Domingo, et al., Dental composites reinforced with hydroxyapatite: mechanical behavior and absorption/elution characteristics, J. Biomed. Mater. Res. 56 (2) (2001) 297–305.
[19] C. Domingo, et al., Hydrolytic stability of experimental hydroxyapatite-filled dental composite materials, Dent. Mater. 19 (6) (2003) 478–486.
[20] A. Wang, D. Liu, H. Yin, Size-controlled synthesis of hydroxyapatite nanorods by chemical precipitation in the presence of organic modifiers, Mater. Sci. Eng. C Mater. Biol. Appl. 27 (2007) 865–869.
[21] W.-H. Lee, et al., A novel approach to enhance protein adsorption and cell proliferation on hydroxyapatite: citric acid treatment, RSC Adv. 3 (2013) 4040–4051.
[22] I.C. Stancu, et al., Synthesis of methacryloyloxyethyl phosphate copolymers and in vitro calcification capacity, Biomaterials 25 (2) (2004) 205–213.
[23] W.-H. Lee, et al., A novel approach to enhance protein adsorption and cell proliferation on hydroxyapatite: citric acid treatment, RSC Adv. 3 (12) (2013) 4040–4051.
[24] O.V. Bustillos, Utilização da técnica de espectrometria de massa na análise de gases oclusos em pastilhas de dióxido de urânio, Dissertação de Mestrado IPEN/CNEN, 1980.
[25] S.C. Moura, et al., Analysis of hydrogen, carbon, sulfur and volatile compounds in (U_3Si_2 - Al) nuclear fuel, INAC 2015: International Nuclear Atlantic Conference Brazilian Nuclear Program State Policy for a Sustainable World, 2015 (Brazil).
[26] R. Osteux, et al., The fixed organic acids of biological media: direct identification by electrochromatography without demineralization, C R Hebd Seances Acad Sci 251 (1960) 1150–1152.
[27] M.C. Rodrigues, et al., Calcium and phosphate release from resin-based materials containing different calcium orthophosphate nanoparticles, J Biomed Mater Res B Appl Biomater 103 (8) (2015) 1670–1678.
[28] S. Allegrini Jr.et al., Amorphous calcium phosphate (ACP) in tissue repair process, Microsc. Res. Tech. 81 (6) (2018) 579–589.
[29] S.V. Dorozhkin, Calcium orthophosphates in dentistry, J Mater Sci Mater Med 24 (6) (2013) 1335–1363.
[30] T. Toshima, et al., Morphology control of brushite prepared by aqueous solution synthesis, Journal of Asian Ceramic Societies 2 (2014) 52–56.
[31] L. Rodriguez-Lorenzo, M. Vallet-Regí, Controlled crystallization of calcium phosphate apatites, Chem. Mater. 12 (2000) 2460–2465.
[32] L. Brecevic, H. Furedi-Milhofer, Precipitation of calcium phosphates from electrolyte solutions. V. The influence of citrate ions, Calcif. Tissue Int. 28 (2) (1979) 131–136.
[33] D. Hanaor, et al., The effects of carboxylic acids on the aqueous dispersion and electrophoretic deposition of ZrO_2, J. Eur. Ceram. Soc. 32 (1) (2012) 235–244.
[34] R.Z. LeGeros, Calcium phosphates in oral biology and medicine, Monogr. Oral Sci. 15 (1991) 1–201.
[35] S. Ahmed, F.R. Jones, A review of particulate reinforcement theories for polymer composites, J. Mater. Sci. 25 (12) (1990) 4933–4942.
[36] J. Leidner, R.T. Woodhams, The strength of polymeric composites containing spherical fillers, J. Appl. Polym. Sci. 18 (6) (1974) 1639–1654.
[37] A.R. Curtis, et al., Water uptake and strength characteristics of a nanofilled resin-based composite, J. Dent. 36 (3) (2008) 186–193.
[38] H.S. Vilela, et al., Effect of calcium orthophosphate: reinforcing glass ratio and prolonged water storage on flexural properties of remineralizing composites, J. Mech. Behav. Biomed. Mater. 104 (2020) 103637.
[39] R.R. Braga, et al., A comparative study between crack analysis and a mechanical test for assessing the polymerization stress of restorative composites, Dent. Mater. 28 (6) (2012) 632–641.
[40] M.W. Beatty, et al., Effect of microfiller fraction and silane treatment on resin composite properties, J. Biomed. Mater. Res. 40 (1) (1998) 12–23.
[41] H.H. Xu, et al., Effect of filler level and particle size on dental caries-inhibiting Ca-PO(4) composite, J Mater Sci Mater Med 20 (8) (2009) 1771–1779.
[42] M.G. Raucci, et al., Effect of citric acid crosslinking cellulose-based hydrogels on osteogenic differentiation, J. Biomed. Mater. Res. A 103 (6) (2015) 2045–2056.
[43] M.D. Weir, et al., Effect of calcium phosphate nanocomposite on in vitro remineralization of human dentin lesions, Dent. Mater. 33 (9) (2017) 1033–1044.